Microstructure and Texture Evolution of Different High Manganese Cast Steels During Hot Deformation and Subsequent Treatment

M.N.S. Lima[1], W.M. Ferreira[2], C.D. Andrade[1], H.F.G. de Abreu[1], J. Klug[1], M. Masoumi[1,*].

[1] Universidade Federal do Ceará, Campus Universitário do Pici – Centro de Tecnologia – Depto. de Engenharia Metalúrgica e de Materiais - CEP: 60440-554 - Fortaleza – CE.
[2] Universidade Federal do Piauí, Campus Universitário Ministro Petrônio Portella –Centro de Tecnologia – Curso de Engenharia Mecânica - CEP:64049-550 - Teresina – PI.
* mohammad@alu.ufc.br

Abstract

Microstructure and texture evolution were studied in two different austenitic high manganese cast steels in each processing condition. Special attention was paid to the effects of hot deformation and subsequent treatment on grain orientation behavior. The roles of Mn and C elements as well as heat treatment processes were investigated by Thermo-Calc. The texture evolutions in the as-cast, solution heat treatment, as-rolled and subsequent treatment were explored via orientation distribution function. The results showed that face-centred cube austenite was developed in steels. Strong {110}<115> texture component was characterized in as-cast in both alloys. Then, the inhomogeneity microstructure and the pronounced microsegregations were removed by annealing and Brass {110}<112>, {110}<111> and {221}<102> components were formed. Finally, cube {001}<100> component was developed during hot rolling in samples.

Keywords: very high carbon steel, high manganese steel, crystallographic texture.

1. Introduction

Carbon is considered as the most important enhance the hardness and strength of steels, even in absence of other alloying elements. This current study focused on the microstructure and texture evolution of ultrahigh carbon steel (more than 1.0 wt.%) steels. The ultrahigh carbon content causes an excessive strength and work-hardening with poor formability, leading to very cleavage and brittle

fracture during deformation even at high temperature [1,2]. Although these materials have an excessive strength and work-hardening, very poor formability is a main determinal factor to use in industries. Continuous demanding of new materials in high pressure-temperature applications also requires the industry to develop new materials with high specific strength and high work-hardening capacity and good formability. To fulfill these requirements, ultrahigh carbon-manganese steels were casted in this work by aiming the Transformation-Induced Plasticity (TRIP) theory [3]. The research effort to characterize the microstructure and texture evolutions under different processing conditions (i.e. as-cast, annealing and hot rolling).

From the crystallographic aspect, shear deformation facilitates dislocation motion across preferred slip systems. It is leading to change in inter-atomic spacing and crystal orientation. The lattice reorientation through heat treatment and deformation is considered as a unique characteristic in crystalline materials. Oh et al. [4] reported that in the high Mn steels with face-centered cubic (FCC) structure the grain orientation takes place on the <111> direction parallel to rolling direction (RD). Rolling of high Mn steels with low stacking-fault-energy (SFE) develops brass {110}<112>, Copper {112}<111> texture components [5,6,7]. It is well-known that the strain energy which is generated during deformation can release by optimizing the grain orientation. Therefore, the main focus of the current work was put on the impact of the microstructure and crystallographic texture obtained in different processing conditions/ routes on the resulting mechanical properties.

2. Experimental

Two type of high-carbo-manganese plates of this work were casted in in the Foundry Laboratory of the Federal University of Ceará (LAF-UFC). The proper elements were melted in vacuum induction furnace protected with Ar gas. Then, the result molten steel cased to plate ingot. The chemical compositions of both alloys are listed in Table 1. For the investigations in this work, as-cast plate with a thickness of 40 mm and a width of 100 mm was cast. The cooling rate was

approximately 150°C/s. To remove the inhomogeneity microstructure and the pronounced microsegregations, the subsequent annealing was applied. In this work, the annealing was conducted at 1000°C for two hours according the Thermo-Calc results based on its chemical composition. Finally, hot rolling was performed at the initial rolling temperature of 1100°C, and at the finishing temperature of around 1000°C. The final hot rolling plate was about 20 mm thick. The plates are then gone through air cooling.

Table1: Chemical composition of both cast steels (wt.%).

	C	Mn	Si	P	S	Ni	Cr	Mo	Cu	Fe
1st alloy	1.17	28.08	0.82	0.030	0.010	0.037	0.088	0.20	0.25	bal.
2nd alloy	1.12	18.92	0.75	0.032	0.009	0.035	0.085	0.18	0.23	bal.

Using the Thermo-Calc software and the TCFE6 database, the phase diagrams of the proposed compositions were constructed as a function of the variation of the C and Mn percentages. Also, the weight fraction diagram of each phase was constructed as a function of temperature. The results of the experimental systems were compared with the commercial steel diagrams.

Microstructural studies carried out using the optical microscopes (Zeiss model, Axio Imager 2) and scanning electron. The samples were ground and polished with diamond paste with a particle size 6, 3 and 1μm. For better preparation of the samples that were subjected to buffing of alumina 0.05 m and further automated final polishing for a period of 5-8 hours per sample in Buehler model 69-1100 1000 minimet device with abrasive silica diluted in distilled water. Then, the sample were etched by 2% Nital solution was applied (2 ml HNO_3 + 98ml ethyl alcohol), for a time of (5/10) seconds, to be followed the grain boundaries of the microstructure. Shortly after another etching was conducted with sodium metabisulphite solution ($Na_2S_2O_5$) dissolved in distilled water in composition (5g Na_2S_2O5 + 50 ml distilled water) for a time (5-10) seconds to be observed dendritic formations of gross microstructure of fusion.

Phase analysis and quantitative texture measurements by means of X-ray diffraction (XRD) were performed using a fully automated texture goniometer that

was operated in back reflection mode at 40kV and 45mA with Co Kα radiation. Four incomplete pole figures {111}, {200}, {220}, and {311} were measured and used for calculation of the orientation distribution functions (ODFs) by using the series expansion method with positivity criterion by Mtex free Matlab toolbox for analyzing and modeling crystallographic textures.

3. Results and discussion

The weight fraction of phase diagram for the both alloys was calculated in accordance with the chemical composition shown in Fig. 1. Computational program Thermo-Calc was aimed to determine the formation of possible precipitated phases during casting and post heat treatments. It is observed that at temperature around 1000°C the cementite and austenite are developed, resulting in elimination the as-cast grain structure with inhomogeneous grain distribution.

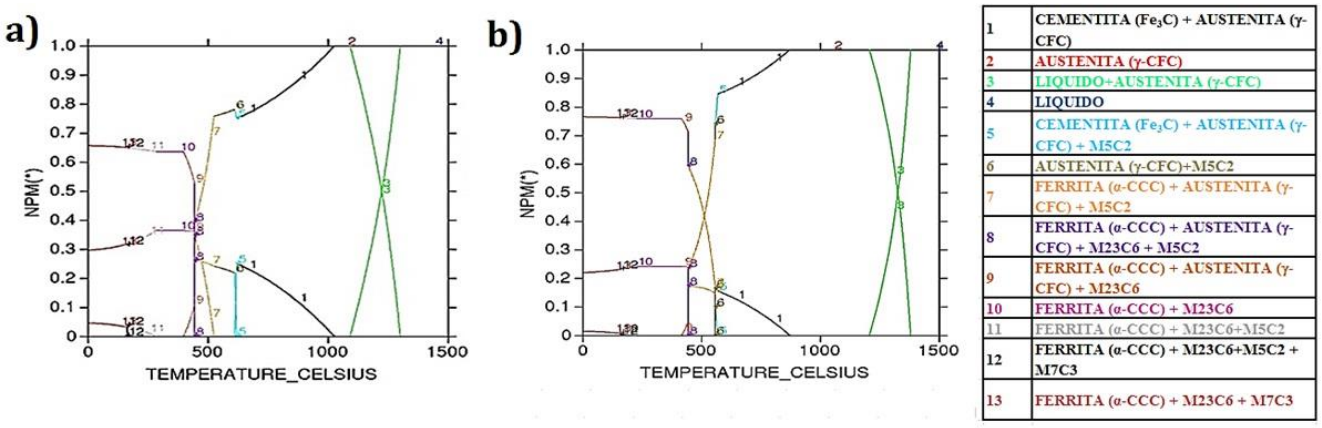

Fig. 1: Weight fraction of phase diagram for the a) 1st alloy and b) 2nd alloy.

It is also shown that in 1st alloy a large amount of carbides also developed such as Mo. However, with a reduction in carbon content and maintaining the high manganese content during austenite stabilizing (i.e. increasing the austenitic phase), the cementite (Fe_3C) microconstituintes reduced significantly. In second alloy, by Fe dissolving, the continues development of FCC structure is observed. It is concluded that the austenite is the final microstructure of both alloys regardless the cooling rate.

Fig. 2 shows the micrographs of as-cast alloys obtained by an optical microscope. A fine dendritic solidification structure with short-wave length microsegregations [8] of alloying elements is characterized by optimal micrographs as shown in Fig. 2. The microstructure shows an inhomogeneous grain structure with comparably large, elongated grains, resulted in a significant anisotropy and poor mechanical properties are indicated from the microstructure. By the comparing of two alloys with different Mn content. It could be concluded that the dendrites and their arm spacing varied with increasing manganese content. These structures which improved by the nucleation and growth of the austenite grain size are affected by the manganese content.

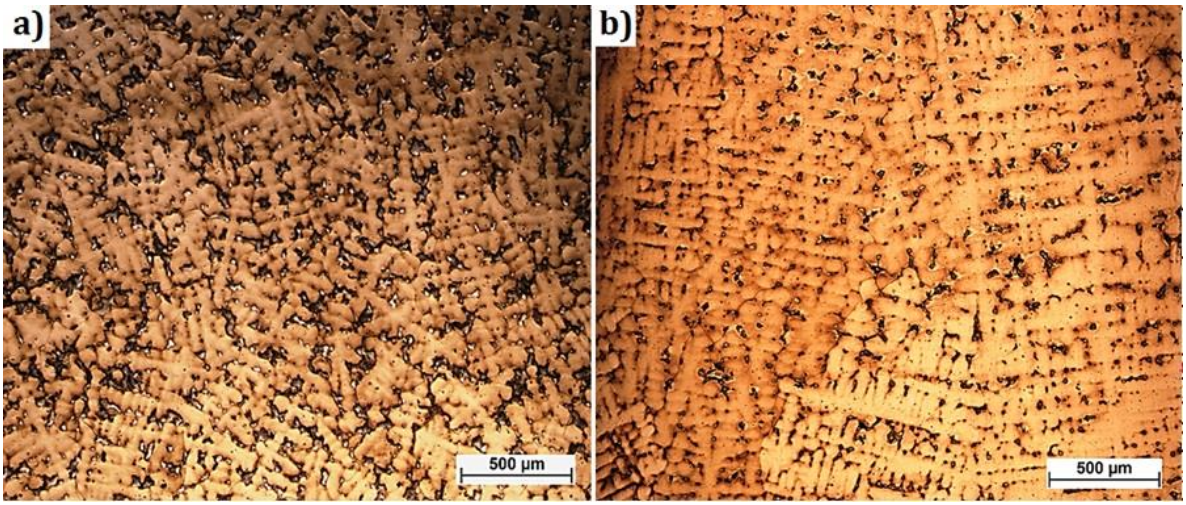

Fig. 2: Dendrites of as-cast alloys a) 1st alloy and b) 2nd alloy.

Fig. 3 shows the microstructure of as-cast sample obtained by optical microscopy. The austenite grains with a large amount of porosities with precipitates are found in these samples. It is observed that air-cooling after casting developed a large number of porosity and voids due to high cooling rate. Thus, removing the undesirable porosities and dissolving the segregations and achieving the desired microstructure with homogenous grain size distribution annealing treatment are required. The second alloy with lower Mn content had coarse austenite grains. The austenite grain sizes are calculated 86±6 and 158±12 µm by Axio Imager 2 installed in Zeiss model optical microscope in both samples, respectively.

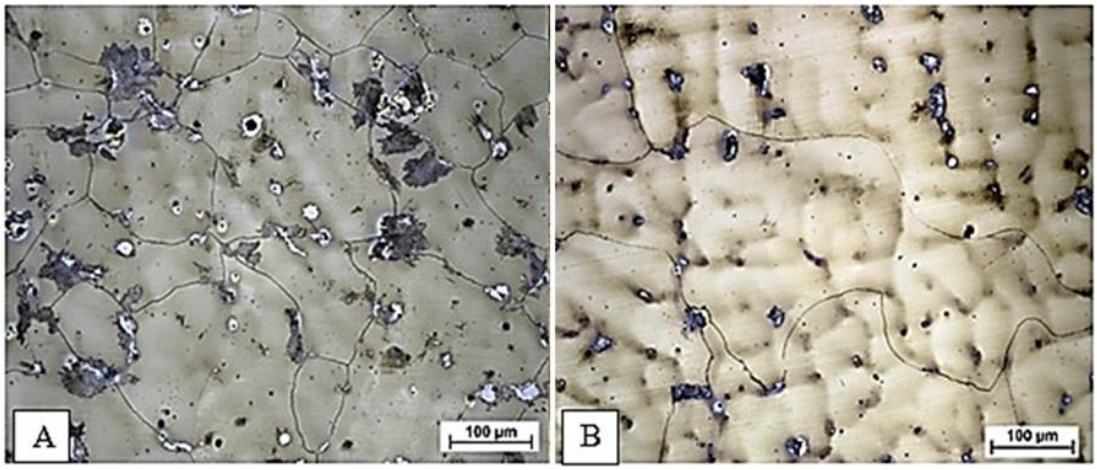

Fig. 3: Micrographs of as-cast alloys a) 1st alloy and b) 2nd alloy.

In order to better and more precious of microstructural studies of as-cast sample, the samples were analyzed by scanning electron microscopy SEM and energy dispersive spectrometer (EDS). The SEM micrographs of as-cast alloys are presented in Fig. 4. The first sample had austenite grains with fine distribution of pearlite microconstituintes were characterized. Moreover, a significant amount of microvoids and precipitates were identified in this sample. The EDS result in this region is presented in Fig. 5a. Carbides and oxides were identified which indicate a poor mechanical properties. The SEM and EDS studies also conducted in second alloy, no pearlite microconstituintes was found, whereas aluminium carbide precipitates developed, Fig. 4b and 5b.

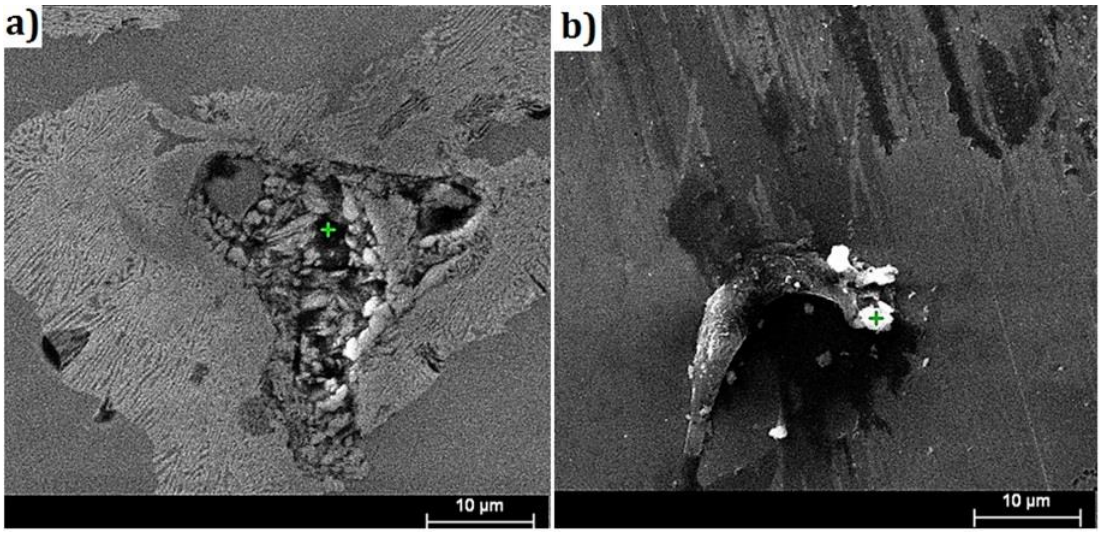

Fig. 4: SEM micrographs of as-cast alloys a) 1st alloy and b) 2nd alloy.

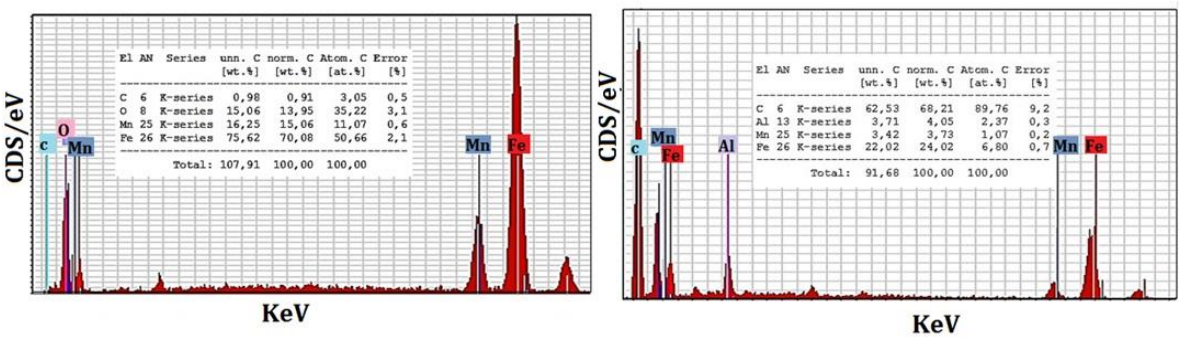

Fig. 5: EDS analyzes of as-cast alloys a) 1st alloy and b) 2nd alloy.

As it was reported, many precipitates such as carbide and aluminium oxide precipitations were identified in as-cast samples of both materials. Nitrogen adsorption isotherms on aluminum oxide samples, is resulting in a very low mechanical properties in compression behaviour. Therefore annealing treatment performed according to results from the computational program Thermo-Calc on 1000°C to eliminate undesirable precipitates and microsegregations. A homogeneous distribution of pearlite microconstituintes in austenite phase is observed in microstructures of both alloys after annealing treatment. Moreover, there no microsegregations were observed in this condition, Fig. 6.

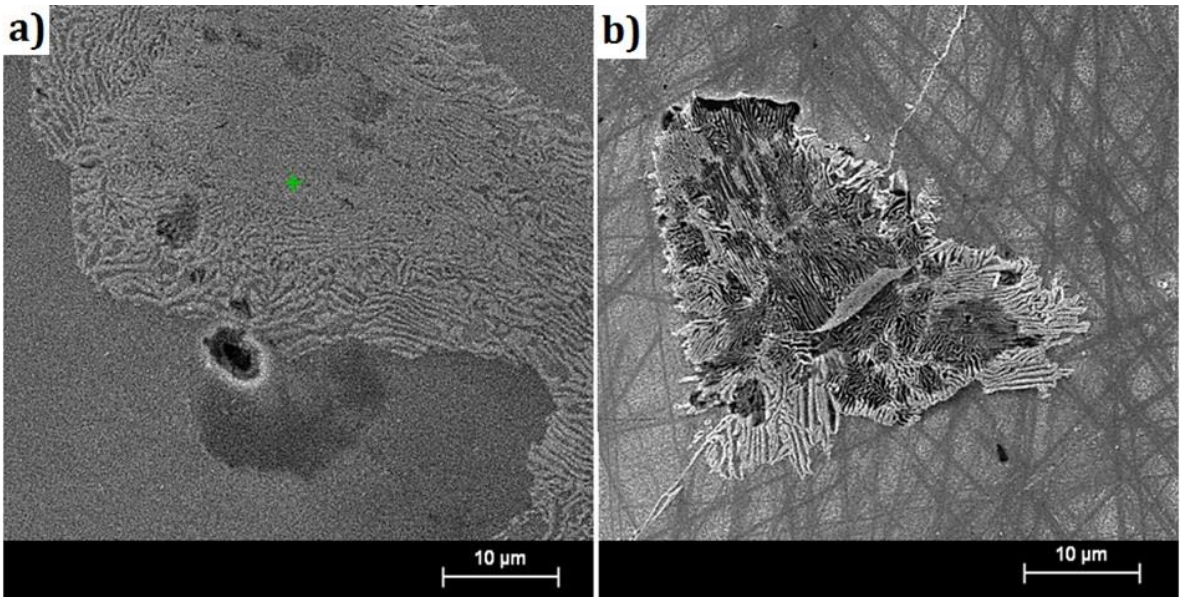

Fig. 6: Fig. 4: SEM micrographs of annealed samples a) 1st alloy and b) 2nd alloy.

The influence of the heat treatment parameters on the microstructural properties, such as grain structure, texture, and element distribution, was analyzed and correlated with the mechanical properties. It is well-known that in the cube structure (i.e. body and face-centered cube) according to the dislocation motion and Taylor factor factory [9]; the grains were laid on compact planes such as {110}, {111} can provide enough slip systems to inaugurate and facilitate deformation [10]. However, the {001} grains (which developed at very high temperatures by phase transformation and recrystallization) due to large atomic distances, poor mechanical properties [11] are achieved.

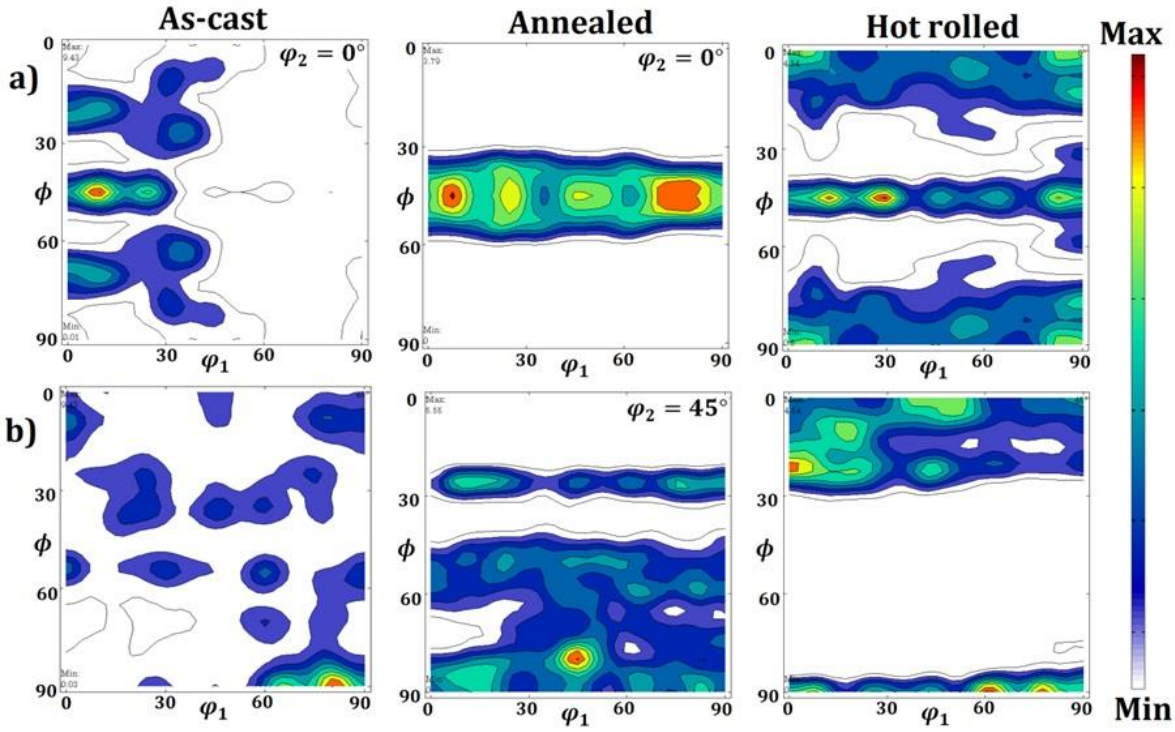

Fig. 7: Calculated ODF in first alloy at a) $\varphi_2 = 0°$ and b) $\varphi_2 = 45°$

In order to investigate texture evolution in alloys, macrotexture analysis was conducted in both samples. Fig. 7 shows the related ODF at $\varphi_2 = 0 \; and \; 45°$ in first alloy. The {110}<115> texture components in as-cast sample, while a large number of porosities and microvoids are leading to early fracture. Brass {110}<112>, {110}<111> and {221}<102> components are characterized in this sample after annealing. This means that the annealing can remove successfully the

inhomogeneous as-cast structure and developed newly organized structure. Then, rotated copper {114}<110> and cube {001}<100> components were formed during rolling at high temperature. High carbon-Manganese steels are considered as low SFE materials [12], thus dynamic recrystallization occurred in these steels during hot deformation. Our findings are fully consistent with mentioned proceed.

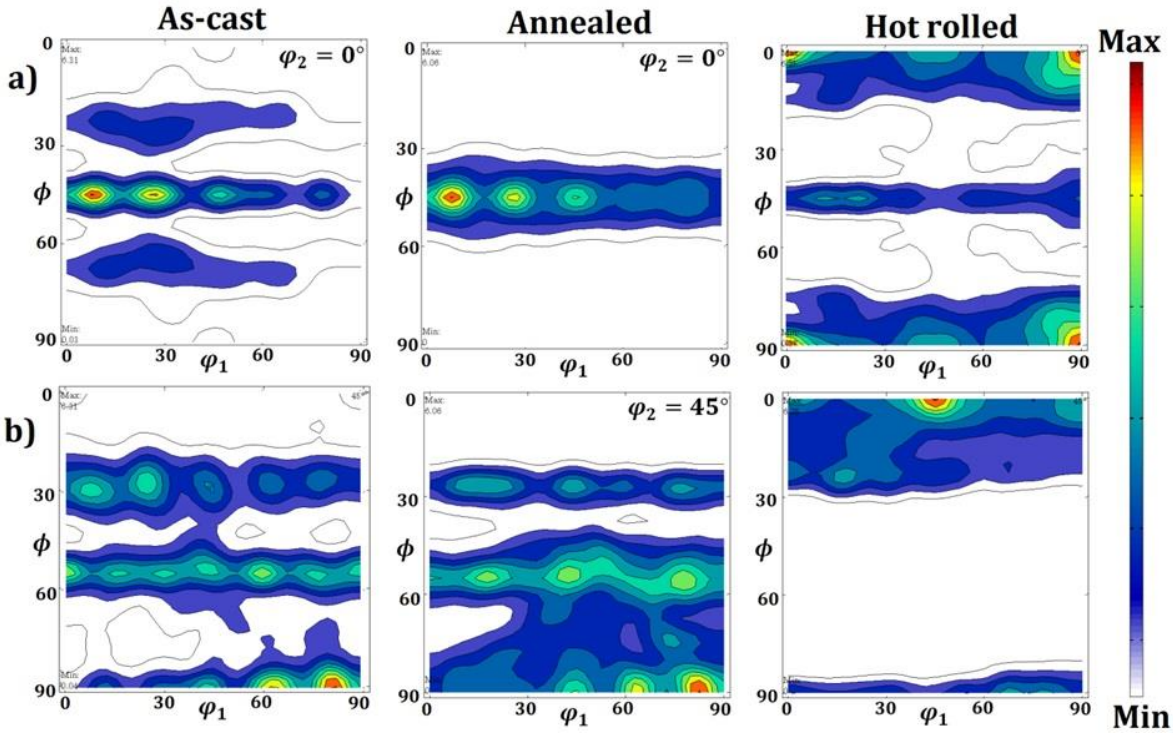

Fig. 8: Calculated ODF in second alloy at a) $\varphi_2 = 0°$ and b) $\varphi_2 = 45°$

Macrotexture investigation was carried out in second alloy of all conditions and their ODFs were calculated and presented in Fig. 8. Besides {110}<115> component that developed in first sample, Brass {110}<112> and {110}<225> texture components also were identified in second sample with lower Mn content. Furthermore, {110}<115>, Brass and {110}<111> components were developed as expected. However, cube {001}<100> component with low mechanical properties were formed significantly in this alloy after hot deformation, because of low SFE and dynamic recrystallization occurrence.

Conclusion

Microstructure and texture evolution were studied in two different austenitic high manganese cast steels in each processing condition. The main focus of the current work was put on the impact of the microstructure and crystallographic texture obtained in different processing conditions/ routes on the resulting mechanical properties. The results revealed that face-centred cube austenite was developed in both alloy steels. Strong {110}<115> texture component was characterized in as-cast in both alloys. Then, the inhomogeneity microstructure and the pronounced microsegregations were removed by annealing and Brass {110}<112>, {110}<111> and {221}<102> components were formed. Finally, cube {001}<100> component was developed during hot rolling in samples.

Acknowledgments

The authors acknowledge the Coordenação de Aperfeiçoamento de Pessoal de Nível Superior (CAPES) for financial support and the research board of the Universidade Federal do Ceará and Laboratório de Caracterização de Materiais (LACAM) for providing the research facilities of this work.

References

1 N.K. Tewary, S.K. Ghosh, Supriya Bera, D. Chakrabarti, S. Chatterjee, Influence of cold rolling on microstructure, texture and mechanical properties of low carbon high Mn TWIP steel, Mat. Sci. Eng. A, 615 (2014) 405-415.

2 K.H. Oh, J.S. Jeong, Y.M. Koo, D.N. Lee, The evolution of the rolling and recrystallization textures in cold-rolled Al containing high Mn austenitic steels, Mat. Chem. Phys. 161 (2015) 9-18.

3 X.G. Wang, L. Wang, M.X. Huang, In-situ evaluation of Lüders band associated with martensitic transformation in a medium Mn transformation-induced plasticity steel, Mat. Sci. Eng. A 674 (2016) 59–63.

4 K.H. Oh, J.S. Jeong, Y.M. Koo, D.N. Lee, Effect of stacking fault energy on formation of deformation twin in high Mn austenitic steel, Mater. Res. Innov. 17 (2013) 73-78.

5 G. Wasserman, Effects of degree and temperature of deformation on texture of silver, Z. Met. 54 (1963) 61-65.

6 J. Hirsch, K. Lücke, Mechanism of deformation and development of rolling textures in polycrystalline fcc metalseI. Acta Metall. 36 (1988) 2863-2882.

7 S. Vercammen, B. Blanpain, B.C. De Cooman, P. Wollants, Cold rolling behaviour of an austenitic Fe-30Mn-3Al-3Si TWIP-steel: the importance of deformation twinning, Acta Mater. 52 (2004) 2005-2012.

8 M. Daamen, C. Haase, J. Dierdorf, D.A. Molodov, G. Hirt, Twin-roll strip casting: A competitive alternative for the production of high-manganese steels with advanced mechanical properties, Mat. Sci. Eng. A 627 (2015) 72-81.

9 J.M. Burgers, W.G. Burgers, Disloca.tions in crystal lattices, Rheology (1956) 141-199.

10 F. Basson, J.H. Driver, Deformation banding mechanisms during plane strain compression of cube-oriented f.c.c. crystals, Act Mat. 48 (2000) 2101-2115.

11 X.P. Chen, X. Chen, J.P. Zhang, Q. Liu, Effect of initial cube texture on the recrystallization texture of cold rolled pure nickel, Mat. Sci. Eng. A 585 (2013) 66-70.

12 R. Xiong, H. Peng, S. Wang, H. Si, Y. Wen, Effect of stacking fault energy on work hardening behaviors in Fe–Mn–Si–C high manganese steels by varying silicon and carbon contents, Mat. Des. 85 (2015) 707-714.